Small Molecule Multi-Targeted Kinase Inhibitor RGB-286638 Triggers P53-Dependent and -Independent Anti-Multiple Myeloma Activity through Inhibition of Transcriptional CDKs

Share Your Story

The Harvard community has made this article openly available.
Please share how this access benefits you. Submit a story .

Accessibility

Small Molecule Multi-Targeted Kinase Inhibitor RGB-286638 Triggers P53-Dependent and -Independent Anti-Multiple Myeloma Activity through Inhibition of Transcriptional CDKs

Diana Cirstea, M.D.[1,2], **Teru Hideshima, M.D., Ph.D.**[2], **Loredana Santo, M.D.**[1], **Homare Eda, M.D.**[1], **Yuko Mishima, M.D.**[1], **Neeharika Nemani, M.S.**[1], **Yiguo Hu, Ph.D.**[2], **Naoya Mimura, M.D., Ph.D.**[2], **Francesca Cottini, M.D.**[2], **Gullu Gorgun, Ph.D.**[2], **Hiroto Ohguchi, M.D., Ph.D.**[2], **Rikio Suzuki, M.D., Ph.D.**[2], **Hannes Loferer, Ph.D.**[3], **Nikhil C. Munshi, M.D.**[2], **Kenneth C. Anderson, M.D.**[2], and **Noopur Raje, M.D.**[1,2]

[1]MGH Cancer Center, Massachusetts General Hospital, Harvard Medical School, Boston

[2]Leebow Institute of Myeloma Therapeutics and Jerome Lipper Multiple Myeloma Disease Center, Dana-Farber Cancer Institute

[3]Agennix AG, Germany

Abstract

Small molecule multi-targeted CDK inhibitors (CDKIs) are of particular interest due to their potent antitumor activity independent of p53 gene alterations. P53 deletion is associated with a very poor prognosis in multiple myeloma (MM). In this regard, we tested the anti-MM activity of RGB-286638, an indenopyrazole-derived CDKI with *Ki*-nanomolar activity against transcriptional CDKs. We examined RGB-286638's mode-of-action in MM cell lines with wild type (wt)-p53 and those expressing mutant p53. RGB-286638 treatment resulted in MM cytotoxicity *in vitro* associated with inhibition of MM tumor growth and prolonged survival *in vivo*. RGB-286638 displayed caspase-dependent apoptosis in both wt-p53 and mutant-p53 cells that was closely associated with the downregulation of RNA polymerase II phosphorylation and inhibition of transcription. RGB-286638-triggered p53 accumulation via nucleolar stress and loss of Mdm2, accompanied by induction of p53 DNA binding activity. Additionally, RGB-286638 mediated p53-independent activity, which was confirmed by cytotoxicity in p53-knockdown and p53-mutant cells. We also demonstrated downregulation of oncogenic miR-19, miR-92a-1, and miR-21. Our data provide the rationale for the development of transcriptional CDK inhibitors as therapeutic agents, which activate p53 in competent cells, while circumventing p53 deficiency through alternative p53-independent cell death mechanisms in p53-mutant/deleted cells.

Keywords

myeloma; p53; transcription; CDKs; apoptosis

INTRODUCTION

Cyclin-dependent kinases (CDKs) are a family of protein kinases that, upon activation by their regulatory cyclin partners, coordinate two main cellular processes which are indispensable for the malignant cell phenotype: cell cycle and transcription[1]. CDK 1, 2, 3, 4 and 6 are key regulators of cell cycle progression[2]. CDKs 4 and 6, complexed with cyclin D, initiate G1 phase-specific transcription by phosphorylating the Rb protein, while CDK2/ cyclin A promotes DNA replication during S phase, and CDK1/cyclin B regulates mitosis. CDK 1, 2, 7, 8, 9 and 11 share important functions in mRNA transcription, and have all been implicated in the phosphorylation of the Ser residues at positions 2 (S^2) and 5 (S^5) of the C-terminal domain (CTD) of the largest RNA polymerase II (RNAPII) subunit essential to RNAPII transcriptional activity[3]. Unlike other CDKs, CDK9 appears to function exclusively on transcriptional regulation, phosphorylates both RNAPII S^2 and S^5, and is critical for transcription elongation of most protein coding genes, including key developmental and stimulus-responsive genes [4].

The rationale for targeting cyclin-dependent kinases (CDKs) and/or cyclins in multiple myeloma (MM) originated from comprehensive cytogenetic studies suggesting that dysregulated and/or increased expression of cyclin D1, D2, or D3 occurs as an early, unifying event in MM pathogenesis, predisposing MM cells to proliferative stimuli[5–7]. In MM, specific inhibition of CDK4/6 by PD 0332991 has demonstrated only growth arrest[8]. Effective MM cytotoxicity was best achieved when multiple CDKs were inhibited concurrently, as with multi-targeted CDK inhibitors such as Seliciclib[9], UCN-01, P276-00[10], and AT7519[11]. In addition to their effect against cell cycle specific cyclins and CDKs, these drugs target transcriptional CDKs, thereby resulting in inhibition/inactivation of RNAPII.

The primary events of RNAPII inactivation in cells are induction of p53 and decreased expression of a number of highly expressed anti-apoptotic proteins with a short half life such as Mcl-1, survivin, and XIAP[12–14]. This may result in both p53-dependent and -independent apoptosis. In MM, p53 deletion has been reported in 10% of newly diagnosed MM tumors, whereas the prevalence is much higher in advanced and extra-medullary tumors, and associates with a very poor prognosis[15, 16]. Hence, CDKIs with activity against transcriptional CDKs, which activate p53 in competent cells, while circumventing p53 deficiency through alternative p53-independent cell death mechanisms in p53-mutant/ deleted cells, are particularly appealing for the treatment of MM.

We examined the anti-MM activity of RGB-286638, a novel compound of the indenopyrazole family of CDKIs with potent cellular activity against transcriptional-type CDKs in MM cells. RGB-286638 mediated RNAPII inhibition, induced p53 accumulation, and triggered cytotoxicity in both wild type (wt)- and mutated-p53 MM cell lines, prompting us to examine RGB-286638's mechanism of action in MM cells expressing wt-p53 versus p53 deficient cells.

MATERIALS AND METHODS

Cell Culture

Dex-sensitive (MM.1S) and -resistant (MM.1R) cells were provided by Dr. Steven Rosen (Northwestern University, Chicago, IL, USA); H929, RPMI8226, and U266 were obtained from ATCC (Rockville, MD, USA); OPM1 plasma cell leukemia cells were provided by Dr. E. Thompson (University of Texas Medical Branch, Galveston, USA). All MM cell lines were cultured in RPMI-1640 containing 10% fetal bovine serum, 2 mM L-glutamine, 100 U/ mL penicillin, and 100g/mL streptomycin. Patient MM primary tumor cells were obtained

from bone marrow (BM) aspirates in accordance with the Declaration of Helsinki, and with the approval of the IRB of Massachusetts General Hospital. BM mononuclear cells were separated using Ficoll-Hipaque density sedimentation, and plasma cells were purified by positive selection with anti-CD138 magnetic activated cell separation microbeads (Miltenyi Biotec, San Diego, CA, USA). BM stroma cells (BMSCs) were generated from BM specimens from MM patients as described previously[17]. Blood samples collected from healthy volunteers were processed by Ficoll-Hipaque gradient to obtain peripheral blood mononuclear cells (PBMCs).

RGB-286638

Was obtained from Agennix USA Inc., Princeton, NJ, USA. For the *in vitro* experiments the drug was provided in 20mg/ml aqueous solution.

5,6-Dichloro-1—D-ribofuranosylbenzimidazole (DRB)

DRB was obtained from Sigma-Aldrich, St. Louis, MO, USA.

Cell Viability Assay

Colorimetric assays were performed to assay drug activity at increasing concentrations of RGB-286638. Cells from 24- or 48-h cultures were pulsed with 10µL of 5mg/mL 3- (4,5-dimethylthiazol-2-yl) -2,5-diphenyl tetrasodium bromide (MTT; Chemicon International Inc, Temecula, CA, USA) to each well, followed by incubation at 37°C for 4h, and addition of 100 µL isopropanol containing 0.04 HCl. Absorbance readings at a wavelength of 570nm (with correction using readings at 630nm) were taken on a spectrophotometer (Molecular Devices Corp., Sunnyvale, CA, USA). All experiments were performed in triplicates.

Western Blotting

MM cells were treated with RGB-286638 and harvested; whole cell lysates were subjected to sodium dodecyl sulfate–polyacrylamide gel electrophoresis (SDS-PAGE) and transferred to nitrocellulose membrane (Bio-Rad Laboratories, Hercules, CA, USA), as described previously[10]. Immunoblotting was performed using specific antibodies: anti-phosphorylated (p)-RNAPII S^2, -p-RNAPII S^5 and -RNAPII (8WG16) (Covance); anti-p-Rb $S^{807/811}$, -p-Rb S^{780}, -p-GSK3 α/β $S^{21/9}$, -GSK3 β, -p-STAT3 S^{727}, -STAT3, -p-GS S^{641}, -p-TAK1 $T^{184/187}$, -p-c-FMS T^{809}, -p-p53 S^{15}, -CDK1, -CDK4, -Cyclin D1, -CDK6, -Cyclin D3, -CDK2, -XIAP, -cleaved caspase 8, 9, and 3, -PARP (Cell Signaling Technology, Beverly, MA, USA); as well as anti-p-ERK1/2, -Cyclin B1, -Cyclin E, -Cyclin A, -Mcl-1, -p53 (DO-1), -Mdm2 (Santa Cruz Biotech, Santa Cruz, CA, USA). Blots were re-probed with the anti-actin (Santa Cruz Biotech), anti-tubulin, or -GAPDH (Cell Signaling Technology) antibodies for equal protein controls.

Cell Cycle Analysis

MM.1S cells (1×10^6) cultured in media alone, or with 50nM RGB-286638, were washed with ice-cold PBS, fixed with 100% ethanol for 1h at 4°C, and pretreated with RNase DNase free (Roche Diagnostics Corporation, Indianapolis, USA) for 30min at 37°C. Cells were stained with PI (5g/mL; Sigma Chemical), and cell cycle profile was determined using the BD Diva software on BD LFR2 flow cytometer (San Jose, CA, USA). Analysis of the data was done using ModFit cell cycle analysis program.

Detection of Apoptosis

Apoptosis detection was performed with the annexin V-PI detection kit (Immunotech/Beckman Coulter). MM.1S cells (1×10^6) were exposed for 12–24h to RGB-286638

(50nM). Cells were then incubated with annexin V-FITC and PI for 15min. Annexin V+PI+ positive apoptotic cells were enumerated using BD LFR2 flow cytometer (San Jose, CA, USA).

MM Xenograft Murine Model

The *in vivo* anti-MM activity of RGB-286638 was evaluated in a previously established MM xenograft model[10]. RGB-286638 dosing solutions of 2 and 3 mg/ml in 5% dextrose/water (D5W) pH5.2, as well as D5W pH5.2 for vehicle control dosing group, were prepared and provided by Agennix AG. CB-17 severe combined immunodeficient (SCID) mice (Charles River Laboratories, Wilmington, MA, USA) were monitored in the Animal Research Facility at DFCI, and subjected to studies approved by the Animal Ethics Committee. Forty male 5–6 week old mice were irradiated (2 Gy [200 rad]) using cesium 137 ($137Cs$)-irradiator source); 24h after irradiation, 2.5×10^6 MM.1S cells were inoculated subcutaneously in the upper back. When tumor weight was approximately 100mg, mice were randomly assigned into 3 cohorts receiving daily IV tail vein injections for 5 consecutive days with either RGB-286638 30mg/kg (8 mice), 40mg/kg (9 mice), or control vehicle alone (10 mice). Animals were monitored for body weight and tumor volume by caliper measurements every alternate day. Tumor volume was estimated using the following formula: $1/2 \times (\text{length}) \times (\text{width})^2$. Animals were euthanized in accordance with DFCI Animal Care and Use Committee guidelines by CO2 inhalation in the event of tumor size > 2cm or due to tumor ulceration. Survival was evaluated from the first day of treatment until death. Tumor growth was evaluated using caliper measurements from the first day of treatment until day of first sacrifice. Percentage tumor growth inhibition (TGI) was calculated as TGI on day X = 100 − T/C% on day X. Log10 cell kill was calculated by the formula $\log 10 \, \text{cell kill} = [\text{tumor growth delay (day)}] \times [\text{tumor doubling time (day)} \times 3.32]$.

RNA Synthesis Assay

Synthesis of RNA was evaluated by measuring the incorporation of [5′-^{3}H]uridine (5μCi/ml) (Perkin Elmer, Boston, MA) into MM.1S, U266, OPM1 and RPMI cells, as described previously[11]. MM cells ($2–3 \times 10^3$ cells/well) were incubated in 96-well culture plates alone or with BMSCs, with varying concentrations of RGB-286638 for 8 or 24 h at 37°C. [5′-^{3}H]uridine was added (1 mCi (37 KBq) per well) prior to harvesting with the automatic cell harvester (Cambridge Technology, Cambridge, MA, USA), then counted using the LKB Betaplate scintillation counter (Wallac, Gaithersburg, MD, USA). [5′-^{3}H]uridine assays were performed in triplicate.

DNA Synthesis Assay

DNA synthesis was measured by tritiated thymidine uptake [^{3}H-TdR] (Perkin Elmer, Boston, MA, USA) as previously described[10, 18]. MM.1S cells ($2–3 \times 10^3$ cells/well) were incubated alone or with BMSCs in 96-well culture plates with varying concentrations of RGB-286638 for 24-, or 48-h at 37°C. Cells were pulsed with [^{3}H-TdR] (0.5 mCi per well) during the last 8h of the end time point, harvested with an automatic cell harvester (Cambridge Technology, Cambridge, MA, USA), and counted by using the LKB Betaplate scintillation counter (Wallac, Gaithersburg, MD, USA). All experiments were performed in triplicates.

RNA Extraction

For miRNA expression profiling, MM.1S cells alone or in co-culture with BMSCs were incubated for 8h in control media or RGB-286638 (50nM). Similarly, MM.1S, OPM1, U266 and RPMI cells were cultured 8h in media alone or 50nM RGB-286638 for miRNA Specific

Assays. Total RNA was extracted from MM cell pellets using *mir*Vana miRNA Isolation Kit (Ambion, Inc), according to the manufacturer's protocol.

miRNA Expression Profiling Using Human TaqMan Low Density Array Cards

miRNA expression profiling was performed on MM.1S cells cultured for 8h in control media or 50nM RGB-286638, with or without BMSCs. TaqMan® Low-Density Array (TLDA) using human miRNA version 2.0A and version 3.0B cards (Applied Biosystems, Foster City, CA, USA) was applied to examine the global change in miRNA expression levels in MM.1S cells when co-cultured with BMSCs, with or without RGB-286638 treatment. A total of 756 mature miRNA updated in the Sanger miRBase v.15.0 were quantified, as previously described [19, 20]. miRNAs with Ct values higher than 35 were excluded from the analysis. Normalization was carried out with the mean of RNU44 and RNU48. Relative quantification (RQ) of miRNA expression was calculated with the $2^{-\Delta\Delta Ct}$ Ct method using the ddCt program.

Real-Time PCR Detection and Quantification of Specific miRNA

To evaluate miR-19, miR-92a-1, and miR-21 expression in p53-wt MM.1S along with p53-mutated U266, RPMI, OPM1 cells with or without 8h RGB-286638 (50nM) treatment, we used target-specific TaqMan® MicroRNA Assays (Applied Biosystems, Foster City, CA, USA), in accordance with the manufacturer's protocols. The $2^{-\Delta\Delta Ct}$ method was used to calculate relative changes in miRNA expression. The results were normalized to levels of miRNA endogenous control (RNU48-001006).

Nucleolar Segregation Analysis

Was performed using The Total Nuclear-ID™ Red/Green Nucleolar/Nuclear Detection Kit (Enzo Life Sciences International, Inc; Plymouth Meeting, PA, USA). Pre-treated with RGB-286638 (50nM) for 3h, MM.1S cells were then incubated with 100μL Dual Detection Reagent for 30 min at 37°C. Live stained cells were analyzed by immunofluorescence microscopy (60X magnification), using a standard FITC filter set for imaging the nucleolus, and a standard Texas Red filter set for the counterstained nucleus.

Sequence Specific P53 DNA Binding Assay

Detection of p53 sequence specific DNA binding activity was performed using the p53 Transcription Factor Assay Kit (Cayman Chemical Company, Ann Arbor, MI, USA) according to the manufacture's protocol. Nuclear proteins were isolated from MM.1S cells treated with 50nM RGB-286638 for 1, 4, and 8 h, using Nuclear Extraction Kit (Affymetrix Inc, Santa Clara, CA, USA). Nuclear protein aliquots were added to the 96-well plate coated with specific double-stranded DNA sequence containing the p53 response element for overnight incubation. p53 in the nuclear extract was detected by addition of a specific primary antibody directed against p53. A secondary antibody conjugated to HRP was added to provide a sensitive colorimetric readout at 450 nm. All experiments were performed in triplicates.

NAD+/NADH Assay

NAD+/NADH quantification assay (BioVision, Mountain View, CA, USA) was performed in MM.1S cultured with RGB-286638 (50nM). A total of 5×10^5 cells were used for the NAD+/NADH extraction. Duplicates of extracted samples (50μL) were transferred into a 96-well plate and incubated at RT for 5min with 100μL of NAD Cycling Mix, to allow the conversion of NAD+ to NADH. Extracted solution (200μL) from each sample was heated at 60°C for 30min for NAD+ decomposition. Duplicates of each NADH sample (50μL) were transferred to a 96-well plate, 10μL/well NADH developing solution was added; after 40min

in the dark, the plate was read at 450nm wavelength on a microplate reader. The ratio of NAD+/NADH was calculated as follows: (NADt – NADH)/NADH.

Lentivirus-Mediated Knockdown of p53

Lentiviral particles expressing shRNA against human TP53 gene (clone name NM_000546.x-941s1c, targeted sequence CACCATCCACTACAACTACAT) were obtained from the Broad Institute (MIT, Boston, MA, USA) and transduced according to the manufacturer's protocol. Briefly, supernatants containing shTP53 or empty vector lentiviral particles were added to exponentially growing MM.1S in media containing polybrene (8μg/ml). Fresh medium was supplemented at 24h after infection. The infectivity was determined after 72h by comparing the differential sensitivity to puromycin (2μg/ml) treatment between parental and transduced cells, as assessed by MTT assay.

RESULTS

RGB-286638 Demonstrated Potent Activity against Transcriptional CDKs in MM Cell Lines and Inhibited Myeloma Cell Growth *in Vitro*

To assess RGB-286638's potential anti-MM activity, we first investigated the *in vitro* effects of RGB-286638 treatment in MM cell lines and primary tumor cells from MM patients. RGB-286638 is a novel compound of the indenopyrazole family of CDK inhibitors (Fig. 1A) that inhibited the kinase activity of cyclin T1-CDK9, cyclin B1-CDK1, cyclin E-CDK2, cyclin D1-CDK4, cyclin E-CDK3, and p35-CDK5 (IC50, 1, 2, 3, 4, and 5 nM, respectively), and was less potent against cyclin H-CDK7 and cyclin D3-CDK6, as demonstrated by *in vitro* kinase profiling[21]. Additionally, RGB-286638 inhibited several tyrosine and serine/threonine non-CDK enzymes, i.e. GSK-3β, TAK1, AMPK, Jak2, MEK1 (Table 1). We investigated the dose- and time-dependent effect of treatment with RGB-286638 (12.5–100nM) on the growth of human p53-wt (MM.1S, MM.1R, and H929) and p53-mutant (U266, OPM1, and RPMI) MM cells by MTT assay, assessing viability at 24 and 48 hours. The half-maximally effective concentrations (EC50) ranged between 20 and 70 nM at 48 hours. Dose-dependent differences in growth among p53-wt and -mutant cells were observed after 50nM treatment, with p53-wt MM.1S, MM.1R and H929 being slightly more sensitive to RGB-286638 treatment at 48h (Fig. 1B). Moreover, RGB-286638 demonstrated equimolar (50nM) activity in freshly isolated tumor cells from MM patients, while manifesting less cytotoxicity in healthy donor PBMCs (Suppl. Fig. S1). Next, we examined RGB-286638 (50nM) activity against transcriptional CDK7/9 and cell cycle-related CDK4/6 in MM cells based on phosphorylation of their RNAPII S^2/S^5 and Rb $S^{780}/S^{807/811}$ substrates, respectively. Using time- and dose-dependent (0–8h; 25–100nM) immunoblot analysis, we found that treatment with RGB-286638 resulted in rapid downregulation of p-RNAPII S^2/S^5 across all tested MM cell lines. RGB-286638 (50nM) reduced the phosphorylation of Rb at $S^{807/811}$ in MM.1S and MM.1R cells, but had no effects on p-Rb S^{780}.

We next evaluated the effects of RGB-286638 treatment on the activity of selective non-CDK enzymes (Suppl Fig. S2). Immunoblot analysis of MM cell lines treated with 50nM RGB-286638 revealed increased phosphorylation of the α subunit of GSK3 at Ser[21], but decreased phosphorylation of β subunit at Ser[9] (Fig. S2-A). Phosphorylated GS at S^{641}, a downstream target of GSK3β, remained unchanged at 4–8h in all cell lines except U266, where it was decreased (Fig. S2-B). Next, 50nM RGB-286638 did not affect the phosphorylation of $T^{184/187}$ residues in the activation loop of TAK1; c-FMS T^{809} phosphorylation was slightly reduced in MM.1R and OPM1 cells (Suppl. Fig. S2-C). We also evaluated RGB-286638 effects on JAK2 and MAPK signaling by examining p-STAT3 S^{727} and p-ERK1/2 in cells exposed to increasing concentrations of RGB-286638 for 4h

(Fig. S2-A). RGB-286638 treatment did not affect STAT3 S^{727}. Moreover, short exposure to RGB-286638 resulted in upregulated p-ERK1/2 in MM.1R, H929, and U266 cells.

RGB-286638-Induced Apoptosis *in Vitro* Translated to Anti-MM Activity *in Vivo*

We next examined the molecular mechanisms underlying RGB-286638-mediated cytotoxicity in p53-wt (MM.1S) and p53-mutant (U266) cells, specifically examining the effects on cell cycle related proteins, and apoptosis. Time-course immunoblot analysis revealed that 50nM RGB-286638 treatment decreased cyclins (A, B1, D1, and D3), CDK1, and CDK4 expression in MM.1S cells, and reduced cyclin A and D1 levels slightly in U266 cells within 8h (Fig. 2A). As expected, 50nM RGB-286638 reduced the expression of the anti-apoptotic proteins Mcl-1 and XIAP. Caspase-8, -9, -3 and PARP cleavage occurred within 4h in both MM.1S and U266 cell lines (Fig. 2B). DNA cell cycle analysis of MM.1S cells treated with RGB-286638 (50nM) revealed G1 and G2/M cell cycle arrest at 12h, followed by sub-G1 fraction at 24h (Fig. 2C). Apoptosis was confirmed by Annexin/PI staining, which demonstrated increased apoptotic MM cells, 25% and 45% at 12 and 24 hours, respectively (Fig. 2D). This *in vitro* RGB-286638-induced MM cytotoxicity translated into effective *in vivo* anti-MM activity in SCID mice xenografted MM.1S cells (Fig. 2E). Dose-finding studies (data not shown) with RGB-286638 identified 40mg/kg/day IV treatment as the maximum tolerated dose in SCID mice. Five days IV treatment with RGB-286638 significantly suppressed MM tumor growth, with maximum TGI (%) noted at day 14 following end of treatment at 85.06% and 86.34% in the 30 mg/kg and 40 mg/kg treated cohorts respectively. The log10 cell kill (LCK Td: 4.5 days) was 1.6 for both treated groups. RGB-286638 treatment was also associated with improved survival, evidenced by first death at day 24 in controls versus day 43 in both treated groups (Fig. 2E lower panel). No toxic deaths occurred during this study: maximum percentage of body weight (BW) loss was observed on day 5 (8.4%) at 30mg/kg dosage schedule, and on day 15 (9.9%) after 40 mg/kg dosing, with weight recovery in the following two weeks.

RGB-286638 Inhibited Transcription

We next investigated effects of RGB-286638 on transcription in MM.1S cells. Since RGB-286638 (50–100nM) reduced RNAPII phosphorylation by 2h (Fig. 3A), and since phosphorylation of the CTD of RNAPII by CDK9/cyclin T is required for transcriptional elongation [22, 23], we assessed the rate of RNA synthesis. Two hours of RGB-286638 (50nM or 100nM) treatment reduced RNA synthesis by 50% (Fig. 3A). Since the BM microenvironment induces transcription and proliferation in MM cells[24, 25], we next examined the effect of treatment on the rate of RNA and DNA synthesis in MM.1S cells, alone or cultured with patient-derived BMSCs. Using RNA synthesis assay, we found that RGB-286638 reduced the total level of transcripts in BMSCs-stimulated MM.1S cells by ~50% at 8h, and ultimately blocked transcription at 24h (Fig. 3B), associated with marked (60%) reduction in DNA synthesis at 8h and complete block of MM.1S proliferation at 24h (Fig. 3C).

RGB-286638 Triggered Stabilization and Activation of p53

Since RGB-286638 inhibited transcription, and since transcriptional inhibitors can induce p53 accumulation via reduction in Mdm2 expression, we next examined effects of RGB-286638 on p53 and Mdm2 expression in MM cells. Time-course western blot analysis of p53-wt (MM.1S, MM.1R, H929) and p53-mutated (U266, OPM1, RPMI) MM cells treated with 50nM RGB-286638 showed decreased Mdm2 expression in all cell lines, associated with upregulated p-p53 S^{15} and p53 levels in p53-wt, but not in p53-mutated, cell lines (Fig. 4A). We next compared the effects of RGB-286638 to the previously described transcription inhibitor DRB on p53 and Mdm2 expression. Similar to RGB-286638, DRB

(2h) significantly inhibited RNA synthesis in MM.1S cells (Suppl. Fig. S3). Western blot studies of MM.1S treated with increasing concentrations of RGB-286638 or DRB for 2h triggered p53 accumulation without affecting Mdm2 levels at doses that inhibited RNAPII phosphorylation and reduced transcription (Fig. 4B).

Previous studies linked nucleolar stress and transcriptional arrest to p53 accumulation. Specifically, transcriptional arrest due to RNA polymerase dephosphorylation triggers nucleolar reorganization and nucleolar segregation[26]. Immunofluorescence microscopy revealed that the nucleoli (green staining) of cells exposed to 3h RGB-286638 treatment formed numerous speckles of fluorescence spread all over the nucleus (red staining) suggesting nucleolar segregation (Fig. 4C). Re-localization of nucleolar compartments during segregation is an energy-dependent repositioning process[27]. We therefore investigated whether RGB-286638 treatment affected the status of nicotinamide nucleotides (NAD/NADH), markers of energy transforming processes. By NADt/NADH quantification assay RGB-286638 treatment resulted in 30% NADt/50% NADH depletion (Suppl. Fig. S4). Western blot analysis of nuclear and cytoplasmic extracts from RGB-286638-treated MM. 1S cells showed accumulation of p-p53 S^{15} and total p53 predominantly in the nuclear compartment (Fig. 4D).

We next examined whether p53 stabilization associated with p53 activation in RGB-286638-treated MM.1S cells. Increased p53 transcriptional activity via enhanced sequence specific DNA binding is essential to p53-dependent apoptosis[28]. P53 sequence specific DNA binding assay evidenced increased p53 DNA binding and transcriptional activation following 4h treatment with 50nM RGB-286638 in MM.1S cells (Fig. 4E). We confirmed this finding in p53-wt MM.1R cells as well (data not shown).

RGB-286638 Mediated p53-Independent Apoptosis in MM Cells

We next tested whether RGB-286638-induced cell death was independent of p53 pathway activation. Knockdown of p53 by p53-targeting shRNA lentiviral constructs rescued 14% cells from RGB-286638-induced cell death (Fig. 5A). No significant effect on p-RNAPII was observed, suggesting that RNAPII activity was independent of p53 status. P53-independent RGB-286638 activity was further validated by its cytotoxic effects in p53-mutated U266, OPM1, and RPMI MM cell lines. As measured by $[5'-^3H]$uridine incorporation, 2h exposure to increasing doses of RGB-286638 reduced RNA synthesis in p53-mutated MM cell lines, with significant inhibition at 24h (Fig. 5B). As expected, western blot studies of p53-mutated U266, OPM1 and RPMI cells showed that RGB-286638 treatment consistently reduced Mcl-1 levels, which preceded PARP cleavage (Fig. 5C).

RGB-286638 Modulated miRNA Expression

RNAPII is a key regulator of miRNA synthesis, and RGB-286638 treatment resulted in early and potent inhibition of RNAPII activity. Moreover, recent studies suggest a strong correlation between dysregulated miRNA and high-risk myeloma[29, 30]. We therefore next examined the effect of the BMSC-MM cell interaction on miRNA. We performed TLDA-based miRNA expression profiling in MM.1S cells cultured for 8h with or without BMSCs, in the presence or absence of 50 nM RGB-286638. Our data demonstrated that RGB-286638 treatment modulated BMSCs-induced miRNA expression (Suppl Fig. S5). Among microarrays identified with significant RQ values, we selected miR-21-3p and miR-19a-5p, which have been associated with tumorigenesis in MM[31–33]. Both were decreased in MM. 1S cells in culture with BMSCs after RGB-286638 treatment as confirmed by miR-21-3p and miR-19a-5p TaqMan Specific miRNA Assays (Fig. 6A).

We next tested the levels of miR-21 and two members of the oncogenic cluster miR-17-92 (miR-19a and miR-92a-1) in p53-mutated MM cells after RGB-286638 treatment. We assayed U266, OPM1, and RPMI cells exposed to RGB-286638 treatment (50nM for 8h) using the TaqMan Specific microRNA assay for miR-21-3p, miR-19a-5p, and miR-92a-1-5p. RGB-286638 treatment significantly reduced miR-21-3p, miR-19a-5p, and miR-92a-1-5p levels in U266 and OPM1 cells (Fig. 6B).

DISCUSSION

It is widely accepted that the diverse effects of CDK inhibitors are due to their activity against multiple CDKs involved in both cell cycle and transcription regulation. Although most clinically evaluated CDK inhibitors target several CDKs, it has been proposed that the induction of apoptosis arises primarily due to inhibition of transcriptional-type CDKs[34]. Inhibition of transcriptional CDKs, in particular CDK9, leads to the downregulation of transcriptionally inducible genes with short half-lives, including cell cycle regulators and anti-apoptotic factors[35].

Our study found CDK9 to be among the primary targets of RGB-286638 mediating its pro-apoptotic activity in MM cells. *In vitro* kinase assays showed that RGB-286638 is a potent inhibitor of CDK 1, 2, 3, 4, 5, and 9; as well as 44- and 55-fold less active against CDK 7 and 6, respectively. Kinase profiling of RGB-286638 identified additional inhibition of distinct serine/threonine and tyrosine protein kinases, predicting modulation of GSK3, STAT3 and MAPK signaling. In MM cells, however, RGB-286638 demonstrated preferential inhibition of CDK9 over other targets. The IC50 of RGB-286638 inhibited MM cell proliferation (50–100 nM) and dephosphorylated RNAPII S^2/S^5, but did not STAT3 modulate phosphorylation of Rb, and ERK1/2 proteins. We noted that p-Rb S^{780} site, which is phosphorylated by several kinases including cyclin D-dependent kinases, was not affected by RGB-286638 treatment. Importantly, $S^{807/811}$ phosphorylation of Rb was targeted by RGB-286638 in MM.1S and MM.1R cells. Recent evidence suggests that physical interaction between CDK9 and Rb is associated with CDK9-mediated phosphorylation of Rb on its C-terminus$^{793–928}$ [36]; therefore, RGB-286638-mediated inhibition of p-Rb $S^{807/811}$ may be triggered by inhibition of CDK9 activity. These findings, together with RGB-286638-induced transcriptional arrest and caspase-dependent apoptosis in MM cell lines, suggest that inhibition of transcriptional CDK, in particular CDK9, is the primary mechanism of action of RGB-286638 in MM cells.

Inhibition of RNAPII-mediated transcription was among the early cellular responses that we detected after RGB-286638 treatment. The blockade of RNA synthesis has been proposed to be an inducer of p53 accumulation[12]. In our study, RGB-286638 treatment increased p53 levels in MM cells in a manner similar to the transcriptional inhibitor DRB. However, the exact molecular mechanisms of inhibited RNAPII and blocked transcription leading to p53 protein stabilization remain unclear. An important trigger seems to be the reduction in Mdm2 mRNA and protein levels[37]. Normally, p53 expression is kept low mainly by interactions with its major regulator Mdm2, which serves as an E3 ubiquitin ligase for p53 and targets p53 for degradation via the 26S proteasome. Hence, depletion of Mdm2 inevitably leads to p53 stabilization and accumulation. We, however, found that RGB-286638-mediated RNAPII inhibition was associated with increased p53 expression before Mdm2 was downregulated, consistent with studies showing that blockade of transcription can induce nuclear accumulation of p53 without downregulation of Mdm2 levels[38]. Specifically, nucleolar fragmentation significantly reduces the levels of 45S precursor ribosomal RNA, leading to increased cellular levels of free ribosomal proteins, some of which (RPL5, RPL11, and RPL23) then bind to the central regulatory domain of Mdm2 protein and inhibit Mdm2-mediated p53 degradation[39–41]. Taken together with our

findings that RGB-286638 treatment induced nucleolar fragmentation, we suggest that nucleolar stress and depletion of Mdm2, both mediated through transcriptional arrest, may contribute to p53 induction in MM cells.

The role of p53 induction in the apoptotic response to CDK inhibitors is controversial. In our study, RGB-286638-induced p53 nuclear accumulation associated with increased p53 DNA binding activity. Increased p53 transcriptional activity via enhanced sequence specific DNA binding is essential to p53-dependent apoptosis[28]. In fact, p53 knockdown rescued 14% cells from RGB-286638-mediated cell death, suggesting p53 played a role in RGB-286638 cytotoxicity. That may in part explain the observed differential response to RGB-286638 between p53-wt and p53-mutant cell lines.

Additionally, RGB-286638 displayed p53-independent cytotoxicity and caspase-dependent apoptosis induction in p53-mutant cells were closely associated with downregulation of RNAPII phosphorylation and inhibition of transcription. RNAPII's control over miRNA transcription, together with recent findings that miR-19, miR-92a-1, and miR-21 miRNAs play a role in MM tumorigenesis, prompted us to examine effects of RGB-286638 on expression of these miRNAs. Our data shows downregulation of oncogenic miR-19, miR-92a-1, and miR-21 associated with reduced expression of Mcl-1 following RNAPII transcriptional arrest in U266 and OPM1 p53-mutant cells, suggesting a contributory effect to p53-independent MM cytotoxicity.

In conclusion, our data provide the rationale for the development of transcriptional CDK inhibitors as anti-MM agents that activate p53 in competent cells, while circumventing p53 deficiency through alternative p53-independent cell death mechanisms in p53-mutant/ deleted cells.

Supplementary Material

Refer to Web version on PubMed Central for supplementary material.

Acknowledgments

BIBLIOGRAPHY

1. Malumbres M, Harlow E, Hunt T, Hunter T, Lahti JM, Manning G, et al. Cyclin-dependent kinases: a family portrait. Nat Cell Biol. 2009; 11(11):1275–6. [PubMed: 19884882]

2. Malumbres M, Barbacid M. Cell cycle, CDKs and cancer: a changing paradigm. Nature reviews Cancer. 2009; 9(3):153–66.

3. Pinhero R, Liaw P, Bertens K, Yankulov K. Three cyclin-dependent kinases preferentially phosphorylate different parts of the C-terminal domain of the large subunit of RNA polymerase II. European journal of biochemistry/FEBS. 2004; 271(5):1004–14. [PubMed: 15009212]

4. Romano G, Giordano A. Role of the cyclin-dependent kinase 9-related pathway in mammalian gene expression and human diseases. Cell cycle (Georgetown, Tex. 2008; 7(23):3664–8.

5. Bergsagel PL, Kuehl WM. Molecular pathogenesis and a consequent classification of multiple myeloma. J Clin Oncol. 2005; 23(26):6333–8. [PubMed: 16155016]

6. Canavese M, Santo L, Raje N. Cyclin dependent kinases in cancer: potential for therapeutic intervention. Cancer Biol Ther. 2012; 13(7):451–7. [PubMed: 22361734]

7. Kramer A, Schultheis B, Bergmann J, Willer A, Hegenbart U, Ho AD, et al. Alterations of the cyclin D1/pRb/p16(INK4A) pathway in multiple myeloma. Leukemia. 2002; 16(9):1844–51. [PubMed: 12200702]

8. Baughn LB, Di Liberto M, Wu K, Toogood PL, Louie T, Gottschalk R, et al. A novel orally active small molecule potently induces G1 arrest in primary myeloma cells and prevents tumor growth by specific inhibition of cyclin-dependent kinase 4/6. Cancer research. 2006; 66(15):7661–7. [PubMed: 16885367]

9. Raje N, Kumar S, Hideshima T, Roccaro A, Ishitsuka K, Yasui H, et al. Seliciclib (CYC202 or R-roscovitine), a small-molecule cyclin-dependent kinase inhibitor, mediates activity via down-regulation of Mcl-1 in multiple myeloma. Blood. 2005; 106(3):1042–7. [PubMed: 15827128]

10. Raje N, Hideshima T, Mukherjee S, Raab M, Vallet S, Chhetri S, et al. Preclinical activity of P276-00, a novel small-molecule cyclin-dependent kinase inhibitor in the therapy of multiple myeloma. Leukemia. 2009; 23(5):961–70. [PubMed: 19151776]

11. Santo L, Vallet S, Hideshima T, Cirstea D, Ikeda H, Pozzi S, et al. AT7519, A novel small molecule multi-cyclin-dependent kinase inhibitor, induces apoptosis in multiple myeloma via GSK-3beta activation and RNA polymerase II inhibition. Oncogene.

12. Ljungman M, Zhang F, Chen F, Rainbow AJ, McKay BC. Inhibition of RNA polymerase II as a trigger for the p53 response. Oncogene. 1999; 18(3):583–92. [PubMed: 9989808]

13. Wang S, Griffiths G, Midgley CA, Barnett AL, Cooper M, Grabarek J, et al. Discovery and characterization of 2-anilino-4- (thiazol-5-yl)pyrimidine transcriptional CDK inhibitors as anticancer agents. Chem Biol. 2010; 17 (10):1111–21. [PubMed: 21035734]

14. Blagosklonny MV, Demidenko ZN, Fojo T. Inhibition of transcription results in accumulation of Wt p53 followed by delayed outburst of p53-inducible proteins: p53 as a sensor of transcriptional integrity. Cell cycle (Georgetown, Tex. 2002; 1(1):67–74.

15. Avet-Loiseau H, Attal M, Moreau P, Charbonnel C, Garban F, Hulin C, et al. Genetic abnormalities and survival in multiple myeloma: the experience of the Intergroupe Francophone du Myelome. Blood. 2007; 109(8):3489–95. [PubMed: 17209057]

16. Jakubowiak AJ, Siegel DS, Martin T, Wang M, Vij R, Lonial S, et al. Treatment outcomes in patients with relapsed and refractory multiple myeloma and high-risk cytogenetics receiving single-agent carfilzomib in the PX-171-003-A1 study. Leukemia. 2013

17. Tai YT, Teoh G, Shima Y, Chauhan D, Treon SP, Raje N, et al. Isolation and characterization of human multiple myeloma cell enriched populations. Journal of immunological methods. 2000; 235(1–2):11–9. [PubMed: 10675753]

18. Scullen T, Santo L, Vallet S, Fulciniti M, Eda H, Cirstea D, et al. Lenalidomide in combination with an activin A-neutralizing antibody: preclinical rationale for a novel anti-myeloma strategy. Leukemia. 2013

19. Mestdagh P, Feys T, Bernard N, Guenther S, Chen C, Speleman F, et al. High-throughput stem-loop RT-qPCR miRNA expression profiling using minute amounts of input RNA. Nucleic acids research. 2008; 36(21):e143. [PubMed: 18940866]

20. Chen Y, Gelfond JA, McManus LM, Shireman PK. Reproducibility of quantitative RT-PCR array in miRNA expression profiling and comparison with microarray analysis. BMC genomics. 2009; 10:407. [PubMed: 19715577]

21. de Bruijn P, Moghaddam-Helmantel IM, de Jonge MJ, Meyer T, Lam MH, Verweij J, et al. Validated bioanalytical method for the quantification of RGB-286638, a novel multi-targeted protein kinase inhibitor, in human plasma and urine by liquid chromatography/tandem triple-quadrupole mass spectrometry. J Pharm Biomed Anal. 2009; 50(5):977–82. [PubMed: 19628352]

22. Palancade B, Bensaude O. Investigating RNA polymerase II carboxyl-terminal domain (CTD) phosphorylation. European journal of biochemistry/FEBS. 2003; 270(19):3859–70. [PubMed: 14511368]

23. Sims RJ 3rd, Belotserkovskaya R, Reinberg D. Elongation by RNA polymerase II: the short and long of it. Genes & development. 2004; 18 (20):2437–68. [PubMed: 15489290]

24. Podar K, Chauhan D, Anderson KC. Bone marrow microenvironment and the identification of new targets for myeloma therapy. Leukemia. 2009; 23 (1):10–24. [PubMed: 18843284]

25. van de Donk NW, Lokhorst HM, Bloem AC. Growth factors and antiapoptotic signaling pathways in multiple myeloma. Leukemia. 2005; 19 (12):2177–85. [PubMed: 16239913]

26. Shav-Tal Y, Blechman J, Darzacq X, Montagna C, Dye BT, Patton JG, et al. Dynamic sorting of nuclear components into distinct nucleolar caps during transcriptional inhibition. Mol Biol Cell. 2005; 16(5):2395–413. [PubMed: 15758027]

27. Sirri V, Urcuqui-Inchima S, Roussel P, Hernandez-Verdun D. Nucleolus: the fascinating nuclear body. Histochemistry and cell biology. 2008; 129(1):13–31. [PubMed: 18046571]

28. Chao C, Saito S, Kang J, Anderson CW, Appella E, Xu Y. p53 transcriptional activity is essential for p53-dependent apoptosis following DNA damage. The EMBO journal. 2000; 19(18):4967–75. [PubMed: 10990460]

29. Pichiorri F, De Luca L, Aqeilan RI. MicroRNAs: new players in multiple myeloma. Frontiers in Genetics. 2011

30. Corthals SL, Sun SM, Kuiper R, de Knegt Y, Broyl A, van der Holt B, et al. MicroRNA signatures characterize multiple myeloma patients. Leukemia. 2011; 25(11):1784–9. [PubMed: 21701488]

31. Loffler D, Brocke-Heidrich K, Pfeifer G, Stocsits C, Hackermuller J, Kretzschmar AK, et al. Interleukin-6 dependent survival of multiple myeloma cells involves the Stat3-mediated induction of microRNA-21 through a highly conserved enhancer. Blood. 2007; 110(4):1330–3. [PubMed: 17496199]

32. Pichiorri F, Suh SS, Ladetto M, Kuehl M, Palumbo T, Drandi D, et al. MicroRNAs regulate critical genes associated with multiple myeloma pathogenesis. Proceedings of the National Academy of Sciences of the United States of America. 2008; 105(35):12885–90. [PubMed: 18728182]

33. Kluiver J, Kroesen BJ, Poppema S, van den Berg A. The role of microRNAs in normal hematopoiesis and hematopoietic malignancies. Leukemia. 2006; 20(11):1931–6. [PubMed: 16990772]

34. Krystof V, Uldrijan S. Cyclin-dependent kinase inhibitors as anticancer drugs. Curr Drug Targets. 2010; 11(3):291–302. [PubMed: 20210754]

35. Krystof V, Baumli S, Furst R. Perspective of cyclin-dependent kinase 9 (CDK9) as a drug target. Curr Pharm Des. 2012; 18(20):2883–90. [PubMed: 22571657]

36. Simone C, Bagella L, Bellan C, Giordano A. Physical interaction between pRb and cdk9/cyclinT2 complex. Oncogene. 2002; 21(26):4158–65. [PubMed: 12037672]

37. Lu W, Chen L, Peng Y, Chen J. Activation of p53 by roscovitine-mediated suppression of MDM2 expression. Oncogene. 2001; 20(25):3206–16. [PubMed: 11423970]

38. O'Hagan HM, Ljungman M. Nuclear accumulation of p53 following inhibition of transcription is not due to diminished levels of MDM2. Oncogene. 2004; 23(32):5505–12. [PubMed: 15094782]

39. Dai MS, Lu H. Inhibition of MDM2-mediated p53 ubiquitination and degradation by ribosomal protein L5. J Biol Chem. 2004; 279(43):44475–82. [PubMed: 15308643]

40. Zhang Y, Wolf GW, Bhat K, Jin A, Allio T, Burkhart WA, et al. Ribosomal protein L11 negatively regulates oncoprotein MDM2 and mediates a p53-dependent ribosomal-stress checkpoint pathway. Molecular and cellular biology. 2003; 23(23):8902–12. [PubMed: 14612427]

41. Dai MS, Zeng SX, Jin Y, Sun XX, David L, Lu H. Ribosomal protein L23 activates p53 by inhibiting MDM2 function in response to ribosomal perturbation but not to translation inhibition. Molecular and cellular biology. 2004; 24(17):7654–68. [PubMed: 15314173]

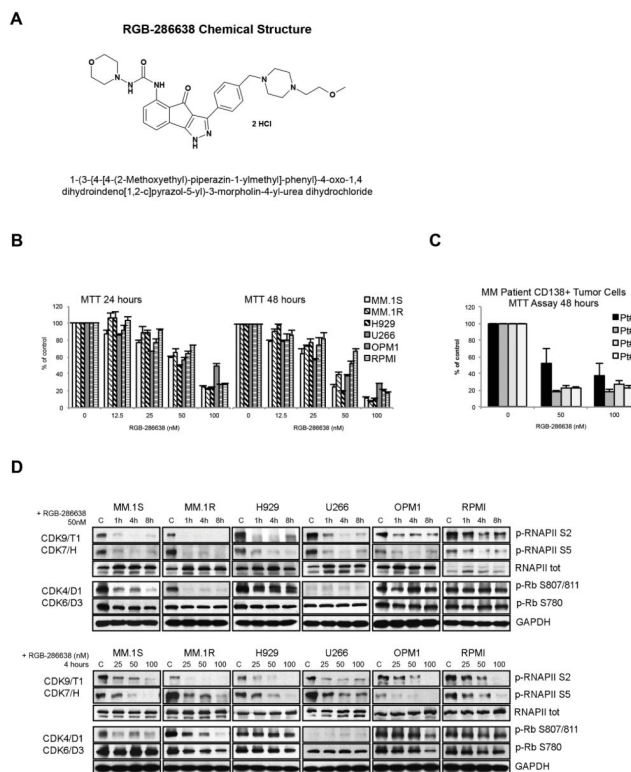**Figure 1. RGB-286638 Demonstrated Potent Activity Against Transcriptional CDKs in MM Cell Lines and Inhibited Myeloma Cell Growth *in Vitro***

(A) RGB-286638 chemical structure (left panel). Chemical name: 1-(3-{4-[4-(2-Methoxyethyl)-piperazin-1-ylmethyl]-phenyl}-4-oxo-1,4-dihydroindeno[1,2-*c*]pyrazol-5-yl)-3-morpholin-4-yl-urea dihydrochloride. Molecular formula: $C_{29}H_{37}N_7O_4$ 2HCl. Molecular weight: 618.52.

(B) Dose- and time-dependent cytotoxicity of RGB-286638 in MM cell lines. Expressing wild-type p53 (MM.1S, MM.1R, H929) or mutant-p53 (U266, OPM1, RPMI) cells were incubated with RGB-286638 (0–100nM), and viability was determined at 24 and 48 h using MTT assay. EC_{50} ranged between 20–70nM at 48h.

(C) RGB-286638-mediated cytotoxicity in primary tumor cells from MM patients. Myeloma cells isolated from BM via CD138+ positive selection were cultured with RGB-286638 (0–100nM), and viability was assessed by MTT at 48h. RGB-286638 demonstrated comparable cytotoxicity to MM cell lines. Data represents means (+/−SD) of triplicate cultures.

(D) RGB-286638 treatment results in transcriptional CDK inhibition. The indicated cell lines were exposed to RGB-286638 (0–100nM) 1, 4, and 8 h treatment. Whole lysates were subjected to western blotting and membranes probed for phosphorylated RNAPII at S^2/S^5 and Rb at $S^{807/811}/S^{780}$ sites using phosphospecific antibodies.
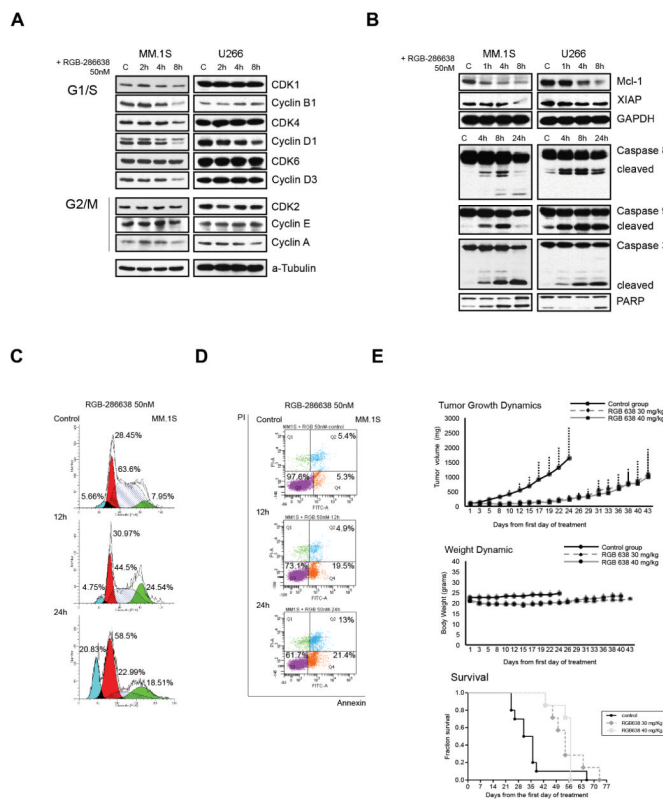
Figure 2. RGB-286638-Induced Cytotoxicity *in Vitro* Translates in Anti-MM Activity *in Vivo*
(A) RGB-286638 reduced the expression of cell cycle related proteins. MM.1S and U266
cells were treated with 50nM RGB-286638 for 2, 4, and 8 h, and whole cell extracts
resolved by SDS-PAGE. Cell cycle-related proteins were assessed through probing
membranes with the indicated antibodies.

**(B) Treatment with RGB-286638 reduced anti-apoptotic protein expression and
triggered caspase and PARP activation.** The expression of RNAPII anti-apoptotic Mcl-1
and XIAP transcripts was examined by western blot in MM.1S and U266 cells treated with
50nM RGB-286638 (0–8h). After 4, 8, and 24 h RGB-286638 (50nM) treatment, MM.1S
and U266 cells were subjected to western blotting for detection of caspase 8, 9, 3 and PARP
cleavage.

(C) RGB-286638 affected cell cycle progression. Cell cycle progression was examined via
flow cytometry in MM.1S cells stained with propidium iodide after exposure to media alone,
or to 50nM RGB-286638 for 12 and 24 h. RGB-286638 treatment affected G1/S and G2/M
cell cycle progression.

(D) RGB-286638 induced early time point apoptosis. Annexin/PI staining and FACS
analysis for apoptosis was performed on MM.1S cells cultured with or without 50nM
RGB-286638 for 12 and 24 h. Viable cells are represented in the lower left quadrants.
Increasing percentages of apoptotic cells after prolonged exposure to RGB-286638
treatment are shown in the lower and upper right quadrants.

**(E) RGB-286638 anti-MM activity *in vivo*: tumor growth, host weight, and Kaplan–
Meier survival curves in xenografted with MM.1S cells mice**. SCID mice were
inoculated subcutaneously with 3×10^6 MM.1S cells in 100 uL RPMI medium. Tumor-
bearing mice were randomly assigned into 3 cohorts receiving daily IV tail vein injections
for 5 consecutive days with 30 mg/kg or 40 mg/kg RGB-286638, or with control vehicle
alone. RGB-286638 treatment resulted in tumor growth inhibition. Transient weight loss,
with maximum body weight loss on day 5 (8.4%) after 30 mg/kg and on day 15 (9.9%) after

40mg/kg dosing, was followed by recovery in the following two weeks. Prolonged survival was observed in both 30 mg/kg and 40 mg/kg dosing groups.
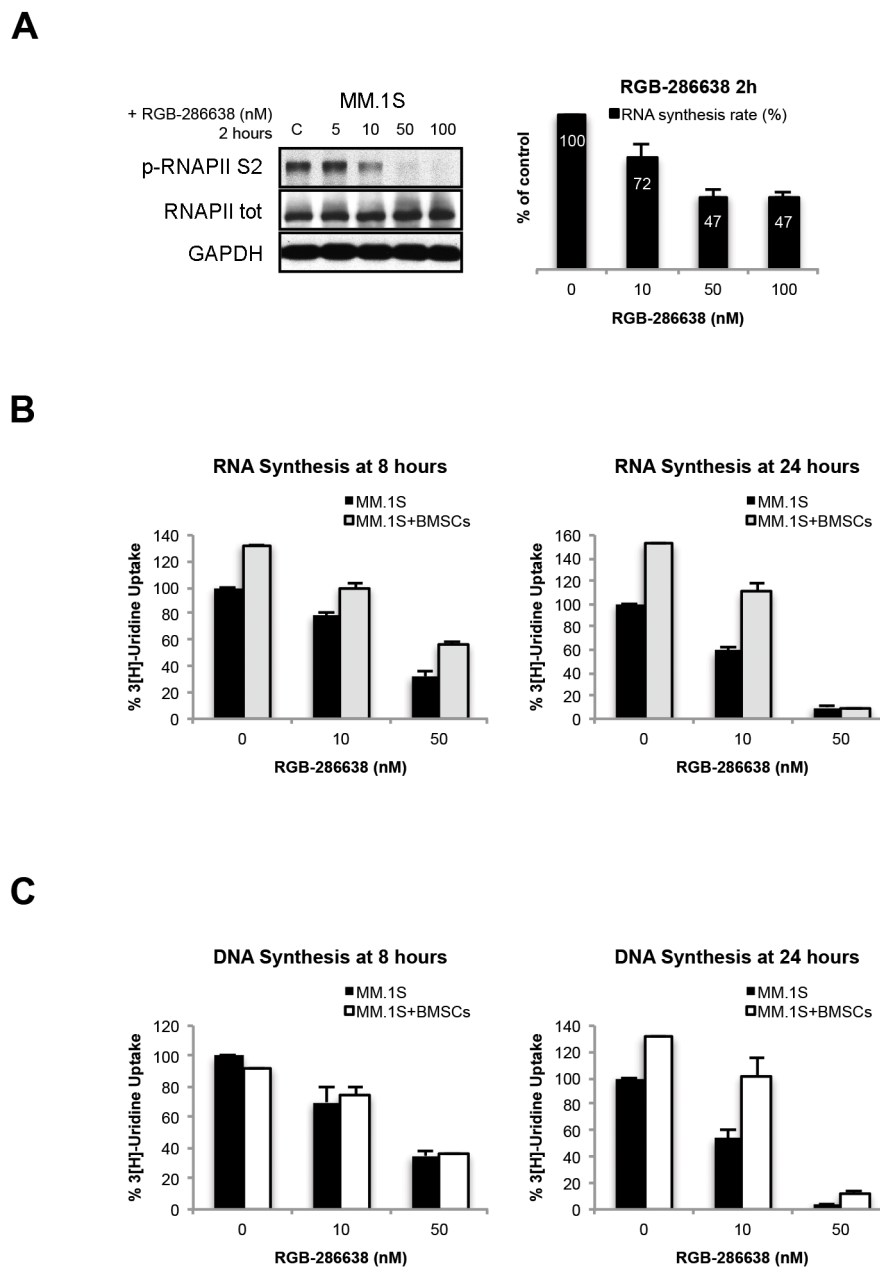
A

B

C

Figure 3. RGB-286638 Inhibited Transcription
(A) RGB-286638 inhibited RNAPII-mediated transcription. MM.1S were incubated with
RGB-286638 (0–100 nM) for 2 hours. Whole cell lysates were subjected to western blotting
and analyzed using specific antibodies for p-RNAPII S^2, RNAPII, and GAPDH. RNA
synthesis was evaluated in MM.1S cells pre-incubated for one hour with the indicated
concentrations of RGB-286638. $[5'-^3H]$uridine was added, and after one hour incubation
cells were assayed for radioactivity. Data represent means (+/−SD) of triplicate cultures.
(B) RGB-286638 reduced BMSC-induced RNA synthesis in MM.1S cells. Cells were
incubated with increasing concentrations of RGB-286638 for 8 and 24 h, alone or in co-
culture with BMSCs; $[5'-^3H]$uridine was added and RNA synthesis measured. Data
represent means (+/−SD) of triplicate cultures.

(C) RGB-286638 abrogated BMSC-induced DNA synthesis in MM.1S cells. MM.1S cells, in the presence or absence of BMSCs, were treated with increasing concentrations of RGB-286638 for 8 and 24 h; cell proliferation was then examined by [^{3}H-TdR] uptake. Data represents means (+/−SD) of triplicate cultures.
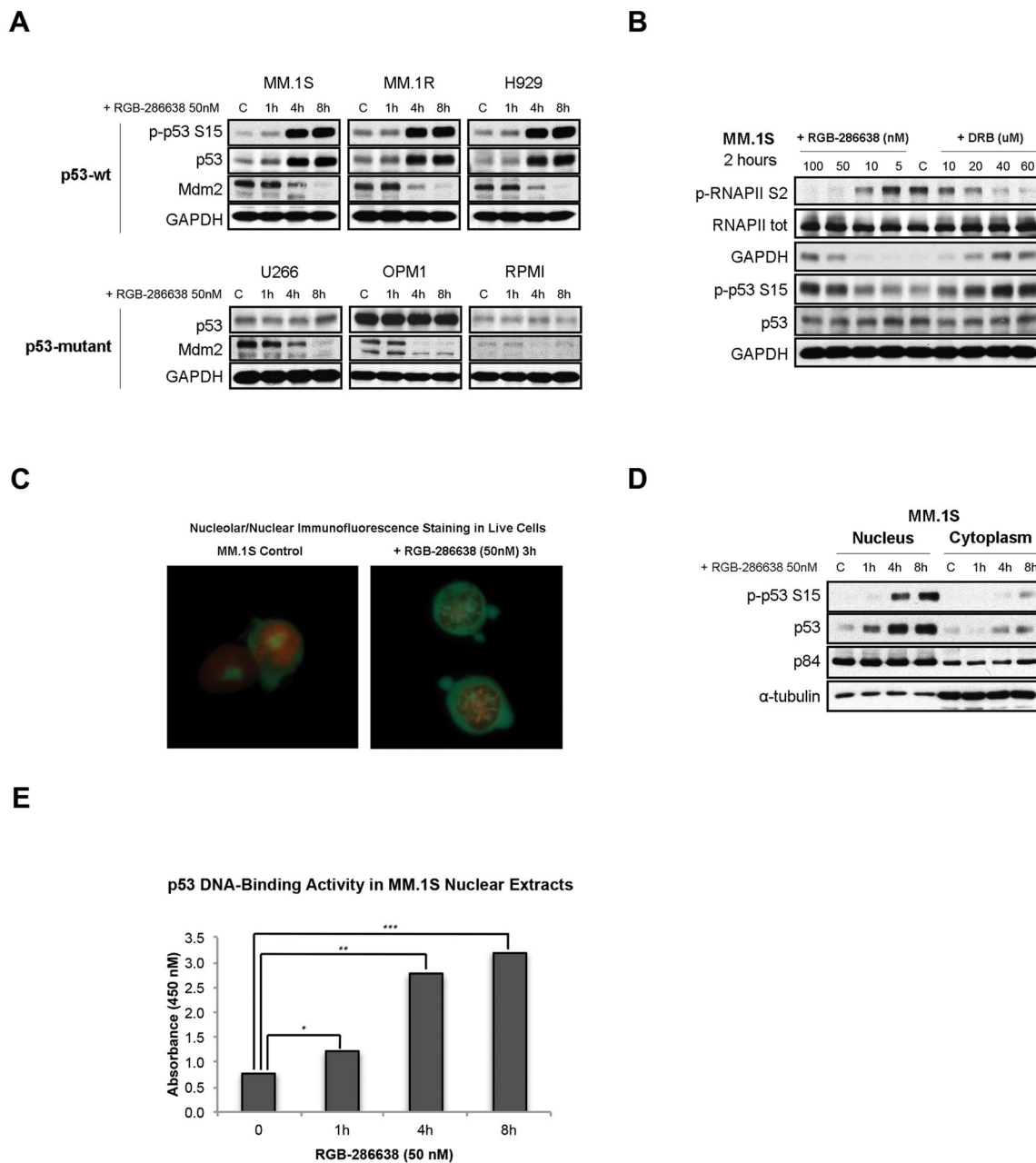
Figure 4. RGB-286638 Triggered Stabilization and Activation of p53

(A) RGB-286638 induced p53 accumulation and reduced Mdm2 expression in wt-p53 MM cells. P53 levels remained unchanged in mutant-p53 MM cells, regardless of reduced Mdm2. Wt-p53 MM.1S, MM.1R, and H929, and mutant-p53 U266, OPM1, and RPMI cells were exposed to 50nM RGB-286638 for 0–8 h, and whole cell extracts then subjected to western blotting. Expression of p-p53 S^{15}, p53, Mdm2, and GAPDH was determined using specific antibodies.

(B) RGB-286638 triggered p53 accumulation prior to reducing Mdm2. p53 and Mdm2 expression were correlated with RNAPII inhibition in MM.1S cells cultured for 2h with control media, or with increasing concentrations of RGB-286638 (0–100nM) or DRB (0–

60uM). Whole cell extracts were examined via western blotting for expression of p-RNAPII S^2, RNAPII, p-p53 S^{15}, p53, and GAPDH.

(C) RGB-286638 induced nucleolar fragmentation. MM.1S cells incubated with RGB-286638 (50nM) or media alone for 3 hours were pelleted and re-suspended in 100 µL Dual Detection Reagent for 30 min. Viable cells were analyzed by immunofluorescence microscopy (60X magnification).

(D) RGB-286638 triggered nuclear accumulation of p53. Nuclear and cytoplasmic extracts separated from MM.1S cells exposed to 50nM RGB-286638 for 0–8 h were analyzed by western blotting for expression of p-p53 S^{15} and p53 using specific antibodies. Expression of p84, or α-tubulin was used for loading control of nuclear or cytoplasmic proteins, respectively.

(E) RGB-286638 increased p53 sequence specific DNA binding activity. P53/DNA binding activity was detected in nuclear extracts purified from MM.1S cells cultured with media, or RGB-286638 (50nM) for 1, 4, and 8 h. Data represents means (+/−SD) of triplicate cultures.
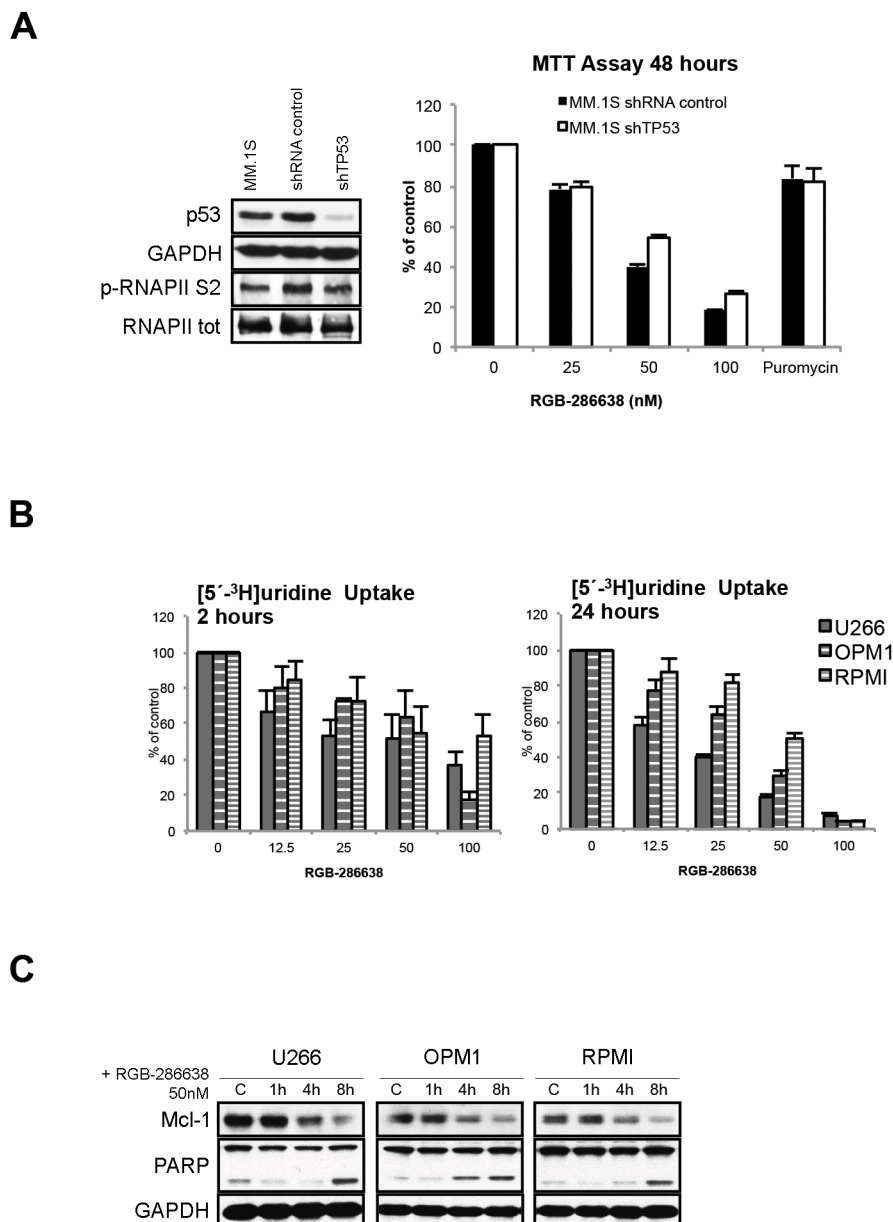
A

B

C

Figure 5. RGB-286638 Mediated p53-Independent Apoptosis in MM Cells
(A) RGB-286638 induced cytotoxicity in p53 knockdown MM.1S. P53 shRNA- or empty vector-transduced MM.1S were cultured with RGB-286638 (0–100nM) or 1.5ug/ml puromycin for 48h, and viability was assayed using MTT. Data represent means (+/−SD) of triplicate cultures. P53 and p-RNAPII S[2] were examined by western blotting of whole cell lysates of parental MM.1S cells and MM.1S cells transduced with p53 shRNA or with empty vector.
(B) RGB-286638 reduced transcription in mutant-p53 MM cell lines. U266, OPM1, and RPMI cells were treated for 2 and 24 h with RGB-286638 (0–100nM); [5′-³H]uridine was then added, and RNA synthesis measured. Data represent means (+/−SD) of triplicate cultures.

(D) RGB-286638 triggered apoptosis in MM cell lines expressing mutant-p53. U266, OPM1, and RPMI cells incubated with or without 50nM RGB-286638 for 1, 4 and 8 h were examined by western blotting with anti-Mcl-1, -PARP, and - GAPDH antibodies.
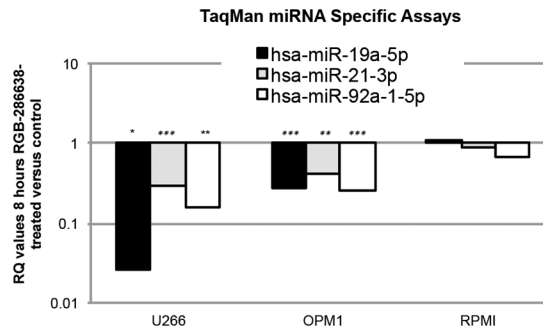
A
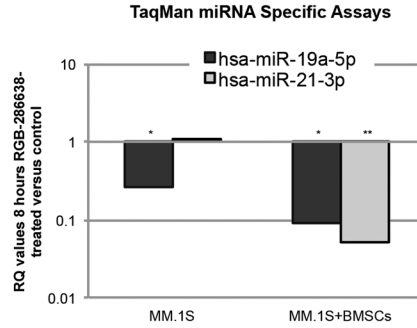
B

Figure 6. RGB-286638 Effects on miRNA Expression
(A) RGB-286638 modulated miRNA expression in MM.1S cells alone and in culture with BMSCs. TaqMan® miR-21-3p and miR-19a-5p miRNA Specific Assays using RT-PCR were performed on aliquots of total RNA extracts from MM.1S cells cultured for 8h in control media or 50nM RGB-286638, with or without BMSCs. Data are presented as relative quantity (RQ) values in RGB-286638 treated versus untreated cells. The experiments were carried out in triplicates, (*) if $p<0.05$ and two (**) if $p<0.01$.
(B) RGB-286638 suppressed the expression of the oncogenic miR-19a-5p, miR-21-3p, and miR-92a-1-5p in mutant-p53 MM cell lines. U266, OPM1, and RPMI cells were incubated in media alone or in 50nM RGB-286638 for 8h. Total RNA extracts were subjected to TaqMan Specific miRNA Assays for miR-21-3p, -19a-5p, and -92a-1-5p detection. Data is presented as RQ values of RGB-286638-treated versus -untreated cells. Experiments were carried out in triplicates, (*) if $p<0.05$ and two (**) if $p<0.01$.

Table 1

RGB-286638 Kinase Profiling

CDKs	IC$_{50}$ (nm)	non-CDKs	IC$_{50}$ (nm)
K9/T1	1	Fms	1
K1/B1	2	GSK-3β	3
K2/E	3	TAK1	5
K4/D1	4	JNK1a1/2	17/40
K3/E	5	C-src	25
K5/p35	5	AMPK	41
K7/H	44	Jak2	50
K6/D3	55	MEK1	54

Note: RGB-286638 multi-targeted kinase activity as measured by in vitro cell-free kinase assays.

Table 1 contains the IC50 kinase inhibition *Ki* (nM) of individual CDKs and selected tyrosine and serine/threonine kinases (determined in biochemical kinase assays).